Hydrogen-Bonded Organic Ferromagnet

Michio M. Matsushita,[†] Akira Izuoka,[†] Tadashi Sugawara,*,[†] Tatsuya Kobayashi,[‡] Nobuo Wada,[‡] Naoya Takeda,[§] and Masayasu Ishikawa[§]

Contribution from the Department of Pure and Applied Sciences and Department of Physics, Graduate School of Arts and Sciences, The University of Tokyo, Komaba, Meguro, Tokyo 153, Japan, and Institute for Solid State Physics, The University of Tokyo, Roppongi, Minato-ku, Tokyo 106, Japan

Received November 25, 1996[⊗]

Abstract: Nitronyl nitroxide derivatives carrying a hydroquinone or a resorcinol moiety 2-(2′,5′-dihydroxyphenyl)-4,4,5,5-tetramethyl-4,5-dihydro-1*H*-imidazolyl-1-oxyl-3-oxide (HQNN) and 2-(3′,5′-dihydroxyphenyl)-4,4,5,5-tetramethyl-4,5-dihydro-1*H*-imidazolyl-1-oxyl 3-oxide (RSNN)) have been designed and prepared. These compounds were found to afford hydrogen-bonded crystals. In the case of HQNN, two phases of crystals (α- and β-HQNN) were obtained. Of these, the crystal structure of α-HQNN is characterized by the intramolecular hydrogen bond between the *o*-hydroxy group and the nitronyl nitroxide and by the intermolecular one-dimensional hydrogen-bonded chain between the *o*- and *p*-hydroxy groups of the neighboring molecules, respectively. Two of the hydrogen-bonded chains run in parallel, and they are connected by the bifurcated hydrogen bonds formed between the *o*-hydroxy groups of the facing molecules in the individual chain. The χT value of this crystal increased monotonously with lowering temperature (ST model, $J = +0.93$ K, $\theta = +0.46$ K) and turned out to exhibit a ferromagnetic phase transition at 0.5 K. On the basis of the heat capacity data, α-HQNN was found to be a three-dimensional ferromagnet. On the other hand, the crystal of β-HQNN was characterized by the intermolecular hydrogen-bonded chain formed between the hydroxy group at the *meta* position and the nitronyl nitroxide and by the interchain $\pi-\pi$ stacking. The magnetic interaction of β-HQNN was interpreted by the ferromagnetic ST model, and this ferromagnetic interaction ($J = +5.0$ K) was accompanied by a weak antiferromagnetic interaction ($\theta = -0.32$ K) at lower temperatures. Although the structural feature of the crystal of RSNN resembles that of the β-HQNN, it exhibited the antiferromagnetic interaction predominantly (ST model, $J = +10.0$ K, $\theta = -4.0$ K). These magnetic behaviors are consistent with McConnell's theory, when the spin densities at the interacting sites connected by hydrogen bonds are taken into account. Thus, it may be concluded that the hydrogen bond plays a role not only in constructing hydrogen-bonded crystals but also in transmitting spin polarization along the hydrogen bond.

Introduction

A current topic in materials science is the construction of novel organic spin systems which are not available from conventional inorganic materials.[1] Discovery of the first genuine organic ferromagnet, *p*-nitrophenyl nitronyl nitroxide (*p*-NPNN),[2] in 1991, stimulated progress in this field and, thereafter, some organic ferromagnets, tetramethyldiazaadamantanedioxyl[3] and benzylideneamino-TMPO,[4] have been reported successively. In particular, the magnetic interaction in *p*-NPNN has been elucidated in detail by means of magnetic

susceptibility, heat capacity, μSR,[5] and neutron diffraction[6] experiments. On the basis of these fortuitous discoveries of organic ferromagnets, it is time to establish methodology for designing organic crystal ferromagnets. A guiding principle concerning intermolecular magnetic interaction among organic radicals, typically for odd alternant hydrocarbons (AHC), is McConnell's theory.[7] The spin distribution of odd AHC is characterized by alternation in signs and magnitudes at each carbon atom.[8] When the spin-distributing π systems interact intermolecularly, it is an energetically favorable mode of overlap where carbon atoms having the opposite spin densities interact. Accordingly, the signs of the largest spin densities of the neighboring molecules should become the same, when the mode of overlap satisfies the topological requirement intermolecularly,[9] leading to the ferromagnetic intermolecular interaction as shown in Figure 1a.

---

* Author to whom correspondence should be addressed.

† Department of Pure and Applied Sciences.

‡ Department of Physics.

§ Institute for Solid State Physics.

⊗ Abstract published in *Advance ACS Abstracts,* April 15, 1997.

(1) For a recent overview, see: Miller, J. S., Dougherty, D. A., Eds. *Mol. Cryst. Liq. Cryst.* **1989**, *176*, 1−562. *Advanced Organic Solid State Materials*; Chiang, L. Y., Chaikin, P. M., Cowan, D. O., Eds.; Materials Research Society: Pittsburgh, PA, 1989; pp 3−92. *Molecular Magnetic Materials*; Gatteschi, D., Kahn, O., Miller, J. S., Palacio, F., Eds.; Kiuwer Academic: Dordrecht, 1991; Vol. A198. Iwamura, H., Miller, J. S., Eds., *Mol. Cryst. Liq. Cryst.* **1993**, *232/233*, 1−360/1−366. Miller, J. S., Epstein, A. J., Eds. *Mol. Cryst. Liq. Cryst.* **1995**, *272*−274. Kollmar, C.; Kahn, O. *Acc. Chem. Res.* **1993**, *26*, 259. Miller, J. S.; Epstein, A. J. *Angew. Chem., Int. Ed. Engl.* **1994**, *33*, 385. Rajca, A. *Chem. Rev.* **1994**, *94*, 871−893. Izuoka, A.; Kumai, R.; Sugawara, T. *Adv. Mater.* **1995**, *7*, 672.

(2) (a) Kinoshita, M.; Turek, P.; Tamura, M.; Nozawa, K.; Shiomi, D.; Nakazawa, Y.; Ishikawa, M.; Takahashi, M.; Awaga, K.; Inabe, T.; Maruyama, Y. *Chem. Lett.* **1991**, 1225. (b) Nakazawa, Y.; Tamura, M.; Shirakawa, N.; Shiomi, D.; Takahashi, M.; Kinoshita, M.; Ishikawa, M. *Phys. Rev. B: Condens. Matter.* **1992**, *46*, 8906.

(3) Chiarelli, R.; Novak, M. A.; Rassat, A.; Tholence, J. L. *Nature* **1993**, *363*, 147.

(4) Nogami, T.; Ishida, T.; Tsuboi, H.; Yoshikawa, H.; Yamamoto, H.; Yasui, M.; Iwasaki, F.; Iwamura, H.; Takeda, N.; Ishikawa, M. *Chem. Lett.* **1995**, 635−636 and references therein.

(5) Le, L. P.; Keren, A.; Luke, G. M.; Wu, W. D.; Uemura, Y. J.; Tamura, M.; Ishikawa, M.; Kinoshita, M. *Chem. Phys. Lett.* **1993**, *206*, 405.

(6) (a) Zheludev, A.; Bonnet, M.; Ressouche, E.; Schweizer, J.; Wan, M.; Wang, H. *J. Magn. Magn. Mater.* **1994**, *135*, 147−160. (b) Zheludev, A.; Ressouche, E.; Schweizer, J.; Turek, P.; Wan, M.; Wang, H. *Solid State Commun.* **1994**, *90*, 233−235.

(7) McConnell, H. M.; *J. Chem. Phys.* **1963**, *39*, 1910.

(8) (a) Hutchison, C. A., Jr.; Kohler, B. E. *J. Chem. Phys.* **1969**, *51*, 3327. (b) Anderson, R. J.; Kohler, B. E. *J. Chem. Phys.* **1978**, *65*, 2451. (c) Teki, Y.; Fujita, I.; Takui, T.; Kinoshita, T.; Itoh, K. *J. Am. Chem. Soc.* **1994**, *116*, 11499−11505.

(9) Izuoka, A.; Murata, S.; Sugawara, T.; Iwamura, H. *J. Am. Chem. Soc.* **1987**, *109*, 2631.
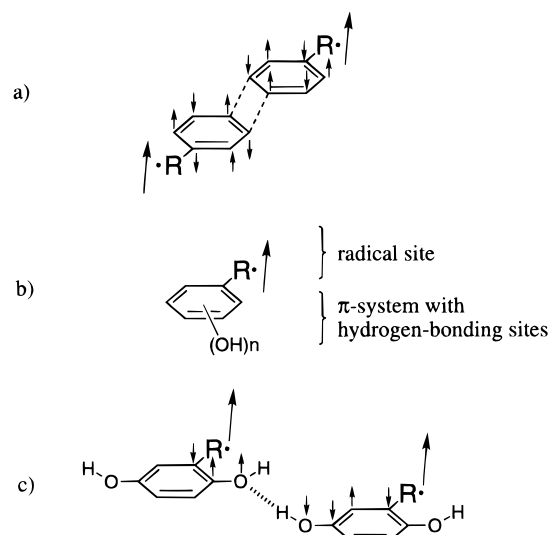

Figure 1. (a) Spin alignment of an odd alternant hydrocarbon based on McConnell's mechanism. (b) Open-shell molecule with hydrogen-bonding sites. (c) Ferromagnetic coupling between open-shell molecules through a hydrogen bond.

In order to realize such a relative orientation, it is crucial to control the molecular arrangement of open-shell molecules in crystals. In this respect, the introduction of a hydrogen-bonding site into an open-shell molecule as an orientation controlling site (Figure 1b) intrigued us because the hydrogen bond leads to a predictable crystal structure.[10] If the hydrogen-bonding sites are spin-polarized, it also plays a role in transmitting the spin-polarization (Figure 1c).[11]

The first hydrogen-bonded organic ferromagnet was reported in 1994 by Sugawara *et al.*[12] This new nitronyl nitroxide derivative, 2-(2′,5′-dihydroxyphenyl)-4,4,5,5-tetramethyl-4,5-dihydro-1*H*-imidazolyl-1-oxyl 3-oxide (HQNN), carries a hy-

HQNN   **RSNN**
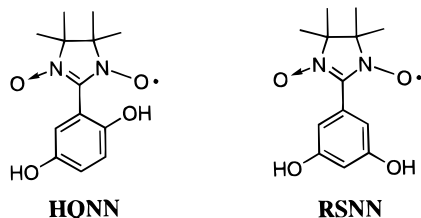
droquinone moiety as hydrogen-bonding site and affords two phases of hydrogen-bonded crystals (α- and β-HQNN). The α-HQNN, in particular, was found to exhibit a ferromagnetic phase transition at 0.5 K. Meanwhile, Veciana *et al.* prepared several derivatives of phenyl nitronyl nitroxide derivatives substituted with hydroxy group(s).[13,14] In 1995, he reported the ferromagnetic phase transition of *o*-hydroxyphenyl nitronyl nitroxide ($T_C = 0.45$ K).[14a] He also documented that utility hydrogen bonds for constructing a magnetically coupled supramolecular structure.

Table 1. ESR *g* Factor, Hyperfine Coupling Constant, OH Stretching Frequency, and Melting Point of α-HQNN, β-HQNN, and RSNN

	ESR[a]			
	g	a_N (mT)	IR (cm^{-1})[b]	mp (°C)
α-HQNN ⎫			3264, 3200-2500 (O-H)	109 (dec)
β-HQNN ⎭	2.0061	0.756	3324, 3200-2500 (O−H)	108 (dec)
RSNN	2.0063	0.748	3312, 3208 (O−H)	75

[a] In benzene solution. [b] KBr pellet.

Table 2. Crystallographic Parameters of α-HQNN, β-HQNN, and RSNN

crystal	α-HQNN	β-HQNN	RSNN
mol wt	265.29	265.29	265.29
space group	$P2_1/n$	$P2_1/a$	$P2_1/n$
a, Å	15.142(3)	10.586(3)	9.817(2)
b, Å	12.320(1)	14.072(2)	19.817(4)
c, Å	7.196(1)	9.744(2)	6.993(1)
β, deg	99.18(2)	113.89(1)	108.07(1)
V, Å^3	1325.3(4)	1327.3(5)	1293.4(4)
Z	4	4	4
T, °C	25	25	25
ρ, g cm^{-1}	1.331	1.333	1.366
no. of reflns	2204	1596	2220
no. of params	240	240	240
R	0.051	0.049	0.047
R_W	0.047[a]	0.048[b]	0.047[c]

[a] | = 1.0 ($|F_o| < 20$), 0.7 ($20 \leq |F_o| < 60$), $200/|F_o|^2$ ($60 \leq |F_o|$). [b] | = 1.0 ($|F_o| < 50$), $200/|F_o|^2$ ($50 \leq |F_o|$). [c] | = 1.0 ($|F_o| < 30$), $500/|F_o|^2$ ($30 \leq |F_o|$).

In this paper, we examined the dimensionality of the magnetic interaction of α-HQNN in detail, based on measurements of the magnetic susceptibility and the heat capacity at cryogenic temperatures. The mechanism of the ferromagnetic interaction was discussed, correlating the data with its crystal structure. Contribution of the hydrogen bond to the transmission of the spin polarization was elucidated using the deuterated sample in reference to the hydroxy groups.[15] Furthermore, the role of the hydrogen bond of α-HQNN in the intermolecular magnetic coupling was discussed, comparing its magnetic data with those of the β-HQNN and of the nitronyl nitroxide derivative, 2-(3′,5′-dihydroxyphenyl)-4,4,5,5-tetramethyl-4,5-dihydro-1*H*-imidazolyl-1-oxyl 3-oxide (RSNN), substituted with a resorcinol moiety.[16]

Results

Molecular Properties of Nitronyl Nitroxides. The synthesis of HQNN and RSNN are described in the Experimental Section. Crystallization of HQNN from ether afforded two phases of crystals (α-HQNN, block-shaped blue-purple crystals; β-HQNN, needle-shaped blue crystals). Crystallization of RSNN from ethyl acetate afforded blue plates. The *g* values and hyperfine coupling constants of HQNN and RSNN in benzene solution are listed in Table 1, together with OH stretching frequencies in IR spectra and melting points.

The Crystal Structures of α-HQNN, β-HQNN, and RSNN. The crystal structures of both phases of HQNN and RSNN were revealed by X-ray crystallography. The crystallographic parameters are listed in Table 2. Molecular structures and selected

(10) (a) Etter, M. C. *Acc. Chem. Res.* **1990**, *23*, 120. (b) Etter, M. C. *J. Phys. Chem.* **1991**, *95*, 4601−4610. (c) Aakeröy, C. B.; Seddon, K. R. *Chem. Soc. Rev.* **1993**, *22*, 397−407.

(11) There are some reports about the magnetic interaction through hydrogen bonds in the transition metal complexes, see: Figgis, B. N.; Kucharski, E. S.; Vrtis, M. *J. Am. Chem. Soc.* **1993**, *115*, 176−18 and references therein.

(12) Sugawara, T.; Matsushita, M. M.; Izuoka, A.; Wada, N.; Takeda, N.; Ishikawa, M. *J. Chem. Soc., Chem. Commun.* **1994**, 1723.

(13) (a) Hernàndez, E.; Mas, M.; Molins, E.; Rovira, C.; Veciana, J. *Angew. Chem., Int. Ed. Engl.* **1993**, *32*, 882. (b) Cirujeda, J.; Hernàndez, E.; Rovira, C.; Stanger, J. L.; Turek, P.; Veciana, J. *J. Mater. Chem.* **1995**, *5*, 243−252. (c) Cirujeda, J.; Ochando, L. E.; Amigó, J. M.; Rovira, C; Ruis, J.; Veciana, J. *Angew. Chem., Int. Ed. Engl.* **1995**, *34*, 55.

(14) (a) Cirujeda, J.; Mas, M.; Molins, E.; Panthou, F. L.; Laugier, J.; Park, J. G.; Paulsen, C.; Rey, P.; Rovira, C.; Veciana, J. *J. Chem. Soc., Chem. Commun.* **1995**, 709. (b) Cirujeda, J.; Hernàndez, E.; Panthou, F. L.; Laugier, J.; Mas, M.; Molins, E.; Rovira, C.; Novoa, J. J.; Rey, P.; Veciana, J. *Mol. Cryst. Liq. Cryst.* **1995**, *271*, 1−12.

(15) Matsushita, M. M.; Izuoka, A.; Sugawara, T. *Mol. Cryst. Liq. Cryst.* **1996**, *279*, 139−144.

(16) The crystal structure and the magnetic property of RSNN have been reported briefly by Veciana *et al.* See ref 14.
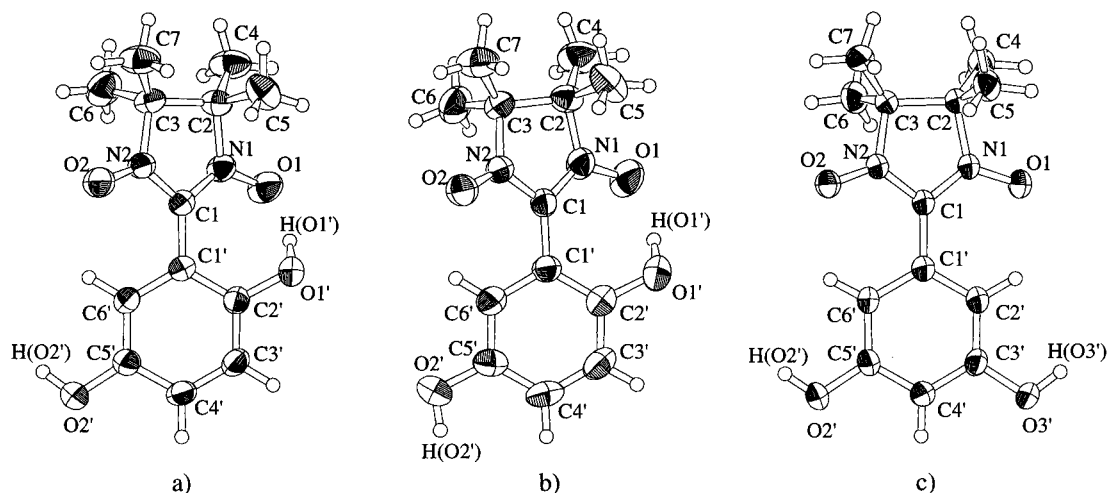
Figure 2. The molecular structure with the atom numbering scheme: (a) α-HQNN, (b) β-HQNN, (c) RSNN.

Table 3. Selected Bond Lengths (Å) and Angles (deg) of α-HQNN, β-HQNN, and RSNN

bonds or angles	α-HQNN	β-HQNN	RSNN
O1−N1	1.303(2)	1.296(4)	1.280(2)
O2−N2	1.272(2)	1.279(4)	1.287(3)
C1−N1	1.332(2)	1.350(5)	1.353(3)
C1−N2	1.367(2)	1.364(5)	1.355(3)
C1−C1′	1.457(3)	1.454(5)	1.464(3)
O1′−C2′	1.367(2)	1.364(5)	1.365(3)
O3′−C3′			1.364(3)
O2′−C5′	1.370(3)	1.376(5)	
O1′−H(O1′)	0.95(3)	0.91(4)	0.84(3)
O2′−H(O2′)	0.89(3)	0.88(6)	
O3′−H(O3′)			0.89(3)
N1−C1−N2	107.7(2)	106.7(3)	107.4(2)
C1−N1−O1	125.7(2)	125.1(3)	126.2(2)
C1−N2−O2	125.9(2)	124.7(3)	125.6(2)
C1−N1−C2	113.0(2)	112.3(3)	112.6(2)
C1−N2−C3	111.5(2)	111.8(3)	112.2(2)
arom ring−O1′−H(O1′)	43(2)	36(3)	5(2)
arom ring−O2′−H(O2′)	4(2)	3(4)	
arom ring−O3′−H(O3′)			13(2)
arom ring−NN plane	37.2(1)	37.2(1)	23.3(1)

bond lengths and angles are given in Figure 2 and Table 3, respectively. Crystal packing of α-HQNN, β-HQNN, and RSNN are shown in Figures 3, 4, and 5, respectively. Geometries of the hydrogen bonds with selected intermolecular contacts of α-HQNN, β-HQNN, and RSNN are summarized in Tables 4, 5, and 6, respectively.

In α-HQNN, an asymmetric unit comprises one molecule and the unit cell contains four molecules with a space group of $P2_1/n$. The phenolic hydroxy group H(O1′) forms a strong intramolecular hydrogen bond (O1′···O1 2.507 (2) Å) with the NN group (N1−O1) (Figure 2 and Table 4). This hydrogen bond causes a bond alternation of the NN group; the O1−N1 and C1−N1 bond lengths at the hydrogen-bonded site are 1.303(2) and 1.332(2) Å, respectively, whereas those of O2−N2 and C1−N2 at the opposite site are 1.272(2) and 1.367(2) Å, respectively, as shown in Table 3. The twist angle around the NN plane and the phenyl ring is 37.2(1)°. The hydroxy group O1′−H(O1′) also participates in an intermolecular hydrogen bond with the O2′−H(O2′) group of the translated molecule along the *c* axis with a distance of 2.752(2) Å (Figure 3a, Table 4). This hydrogen bond forms a one-dimensional hydrogen-bonded chain, consisting of HQNN molecules. A similar one-dimensional chain runs in parallel with inversion symmetry between the two facing molecules (Figure 3b). Two facing NN

groups in the parallel hydrogen-bonded chain are located in proximity to each other with the NO···ON distance of 3.159-(2) Å as shown in Figure 3c and Table 4. The situation is presumably derived from the bifurcated hydrogen bond formed by the two facing phenolic hydroxy groups and the NN groups. These two doubly hydrogen-bonded chains are arranged in a herringbone-type structure as depicted in Figure 3d. There are CH···ON type contacts with the distance of 3.11(3) Å between the methyl proton and the NO group of the adjacent molecule as shown by dashed lines (Table 4).

The unit cell of the β-phase crystal of HQNN contains four crystallographic equivalent molecules with a space group of $P2_1/a$ as in the case of the α-phase. The phenolic hydroxy group at 2′-position participates in the intramolecular hydrogen bond with the oxygen atom of the NN group (Figure 2). The intramolecular O1−O1′ distance of 2.616(6) Å is slightly longer than that of α-HQNN (Table 5). As a result, the degree of bond alternation in the NN group is lessened to some extent: O1−N1, 1.296(4) Å, C1−N1, 1.350(5) Å, O2−N2, 1.279(5) Å; C1−N2, 1.364(5) Å, respectively (Table 3). The twist angle between the NN plane and the phenyl ring is 37.2(1)° and is almost the same as that of α-HQNN.

The phenolic hydroxy group at 5′-position of β-HQNN also forms the intermolecular hydrogen bond. The acceptor of the intermolecular hydrogen bond, however, is not the phenolic oxygen, but the oxygen atom of the NN group which does not participate in the intramolecular hydrogen bond (Figure 4a). Namely, the hydroxy group forms an intermolecular hydrogen bond with the NO group of the adjacent molecule ($x + 1/2$, $−y + 5/2$, z), the intermolecular O2···O2′ distance being 2.777(4) Å (Table 5). The hydrogen-bonded chain runs in a zigzag manner along the *a*-axis. Such hydrogen-bonded chains stack along the *c*-axis. The HQNN molecules in the stack are dimerized as shown in Figure 4b. Within the dimer, HQNN has the inversion symmetry with the molecules represented by ($−x + 1$, $−y + 2$, $−z + 1$). The oxygen atom of the NN group is close to the C(1) of the NN group (3.781(4) Å) of the molecule above, *vice versa*, shown as an overlap mode A in Figure 4c. On the other hand, interatomic distances of the NN groups between dimers of mode B (Figure 4c) are longer than 4 Å.

In the crystal of RSNN,[16] the unit cell contains four crystallographically equivalent molecules with a space group of $P2_1/n$. There is no bond alternation in the NN group due to the lack of an intramolecular hydrogen bond (Table 3). The twist angle between the NN plane and the phenyl ring is 23.3(1)°, and it is smaller than that of HQNN. In this crystal,
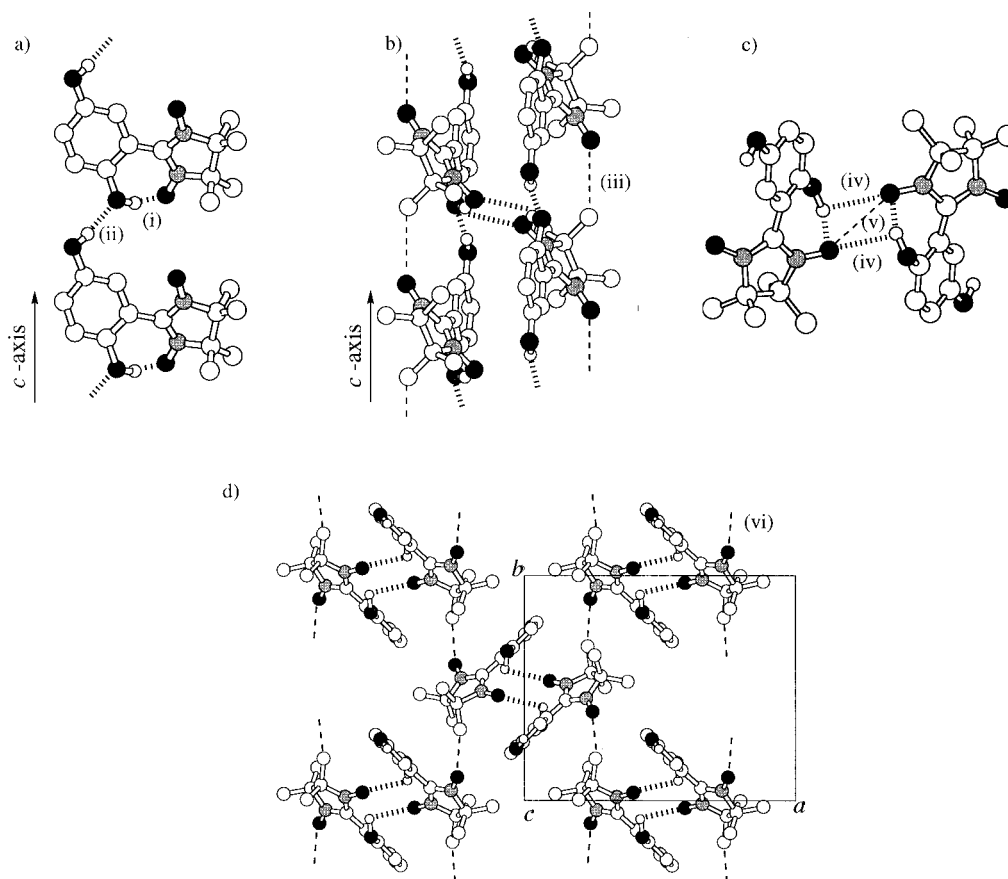
Figure 3. Crystal structure of α-HQNN: (a) Hydrogen-bonded array along the *c*-axis, (b) Facing hydrogen-bonded arrays connected by bifurcated hydrogen bonds, (c) Bifurcated hydrogen-bonded pair, (d) Projected figure along the *c*-axis. Dashed lines show the N−O···H−C contact within the *ab*-plane.
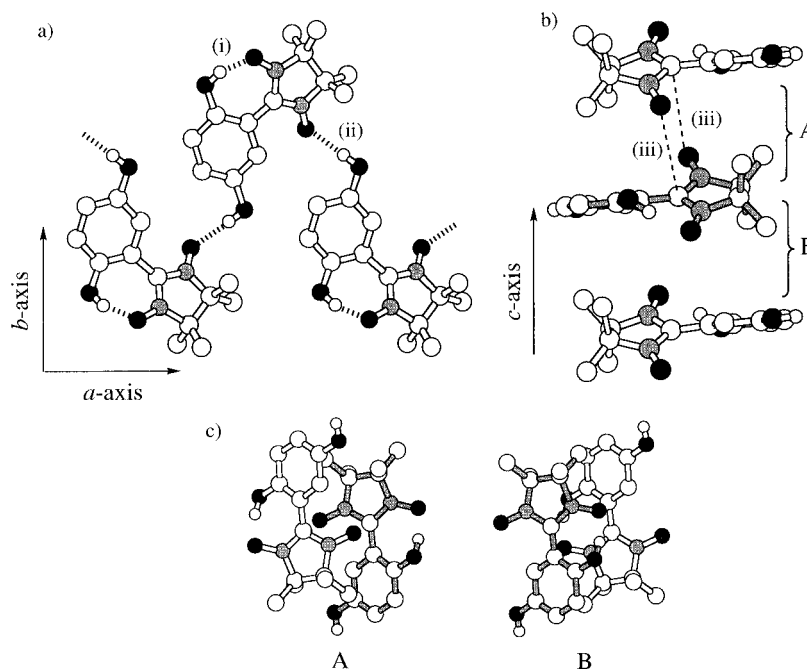

Figure 4. Crystal structure of β-HQNN: (a) Hydrogen-bonded chain along the α-axis, (b) Molecular stack along the *c*-axis, (c) Two modes of overlap within the molecular stack.

the hydroxy groups at 3′- and 5′-positions are hydrogen-bonded intermolecularly with the oxygen atoms of the NN groups of two adjacent molecules at both sites. They are related by the inversion symmetry (Figure 5a). Both of the oxygen atoms of the NN groups of RSNN, in turn, are hydrogen bonded by hydroxy groups of the adjacent molecules. Thus, the RSNN molecules are doubly hydrogen-bonded with each other, forming

a hydrogen-bonded chain along the −1 0 1 direction. This hydrogen-bonded chain is slightly dimerized. While the distances of the hydrogen bonds are the same on one side of the molecule, they are slightly longer on the other side (Table 6). The hydrogen-bonded chains are stacked along the 1 0 1 direction (Figure 5b). Since the stacking is dimerized, there are two types of overlapping modes as depicted in Figure 5c.
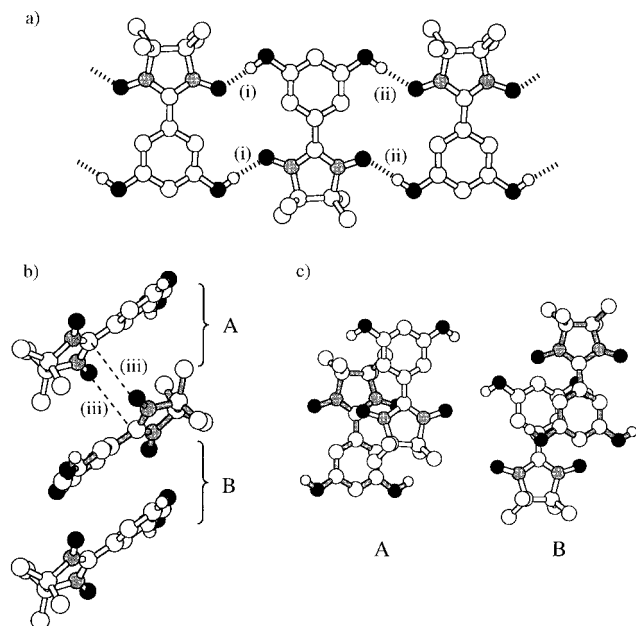
a)

b)

c)

A

B

A　　　　　B

Figure 5. Crystal structure of RSNN: (a) Hydrogen-bonded chain along the −1 0 1 direction, (b) Molecular stack along the 1 0 1 direction, (c) Two modes of overlaps within the molecular stack.

Table 4. Intermolecular Distances of α-HQNN[a]

contact	D−H⋯A	$r(H\cdots A)$, Å	$r(D\cdots A)$, Å	$\angle(D-H\cdots A)$, deg
3-i	O1′−H(O1′)⋯O1	1.59(3)	2.507(2)	161(3)
3-ii	O2′−H(O2′)⋯O1′*	1.87(3)	2.752(2)	170(1)
3-iii	C5−H(C5)⋯O2*	2.78(3)	3.580(3)	140(1)
3-iv	O1′−H(O1′)⋯O1**	2.68(3)	2.999(2)	101(1)
3-v	O1⋯O1**		3.159(2)	
3-vi	C4−H(C4)⋯O2***	3.11(3)	3.679(3)	109(1)

[a] Symmetry code: (*) $x, y, z + 1$; (**) $-x, -y, -z + 1$; (***) $-x + \frac{1}{2}, y + \frac{1}{2}, -z + \frac{3}{2}$.

Table 5. Intermolecular Distances of β-HQNN[a]

contact	D−H⋯A	$r(H\cdots A)$, Å	$r(D\cdots A)$, Å	$\angle(D-H\cdots A)$, deg
4-i	O1′−H(O1′)⋯O1	1.73(4)	2.616(6)	165(4)
4-ii	O2′−H(O2′)⋯O1*	1.90(6)	2.777(4)	176(2)
4-iii	O2⋯C1**		3.781(4)	

[a] Symmetry code: (*) $x + \frac{1}{2}, -y + \frac{5}{2}, z$; (**) $-x + 1, -y + 2, -z + 1$.

Table 6. Intermolecular Distances of RSNN[a]

contact	D−H⋯A	$r(H\cdots A)$, Å	$r(D\cdots A)$, Å	$\angle(D-H\cdots A)$, deg
5-i	O1′−H(O1′)⋯O1*	1.84(3)	2.742(2)	176(1)
5-ii	O3′−H(O3′)⋯O2**	1.89(3)	2.782(2)	177(1)
5-iii	O2⋯C1***		3.727(2)	

[a] Symmetry code: (*) $-x + 2, -y + 1, -z$; (**) $-x + 1, -y + 1, -z + 1$; (***) $-x + 1, -y + 1, -z$.

The oxygen of the NN group (O2) is located close to the C1 of the NN group of the dimeric counterpart with the intermolecular distance of 3.727(2) Å in mode A of Figure 5c (Table 5). Since the overlap of the NN groups between the dimers (mode B) is poor, the NN groups are located remote from each other.

Magnetic Property of α-HQNN, β-HQNN, and RSNN. The χT values for the polycrystalline samples of α-HQNN, β-HQNN, and RSNN are depicted in Figure 6. The χT values of the three samples at room temperature were 0.383, 0.381, and 0.377, respectively. Since these values were close to the χT value for the independent $S = \frac{1}{2}$ spin, the purity of the
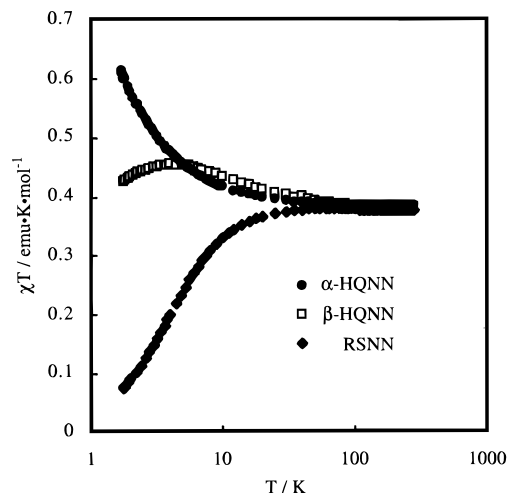

Figure 6. Temperature dependence of the magnetic susceptibility of α-HQNN, β-HQNN, and RSNN.

Table 7. Exchange Interaction (J) of a Dimeric Pair and Weiss Temperature (θ) of α-HQNN, β-HQNN, and RSNN

compd	J_{ST}/k_B, K	θ, K
α-HQNN	+0.93(3)	+0.46(2)
β-HQNN	+5.0(1)	−0.32(1)
RSNN	+10(1)	−4.0(2)

samples was assured. The χT values of α-HQNN increased monotonously in the entire temperature range measured. The temperature dependence of the magnetic susceptibility of α-HQNN was well reproduced by the ST model ($J/k_b = 0.93$ K) with a positive Weiss temperature of $\theta = +0.46$ K (eq 1).

$$\chi = \frac{Ng^2\mu_B^2}{k_B(T - \theta)} \frac{1}{3 + \exp(-2J/k_BT)} \tag{1}$$

While the experimental plot for β-HQNN also increased with lowering temperature, the χT value started to decrease at temperatures lower than 3 K, exhibiting an antiferromagnetic interaction. The plot was found to be best fitted by the ST model with the ferromagnetic intradimer exchange interaction of $J/k_b = 5.0$ K with a negative Weiss temperature of $\theta = -0.32$ K. The plot for RSNN[16] was also reproduced by the ST model with the ferromagnetic intradimer exchange interaction of $J/k_b = 10$ K with a negative Weiss temperature of $\theta = -4.0$ K. The magnetic parameters of all samples are summarized in Table 7.

Magnetic Property of α-HQNN at Lower Temperatures. The ac susceptibility of α-HQNN increased rapidly around 0.5 K (Figure 7), suggesting that a phase transition to the ferromagnetic phase occurred at this temperature. Incidentally, the magnetization at temperatures lower than the transition temperature changed irregularly with lowering the temperature. To clarify the nature of the low-temperature phase, the magnetization curve above and below T_C was measured. Although the magnetization at 733 mK was dependent linearly on the external magnetic field, the magnetization curve at 80 mK exhibited a rapid saturation at 100 Oe (Figure 8). Since the estimated saturation value of the magnetization was very close to the theoretical value (1 $m_B \cdot mol^{-1}$), the phase transition could be regarded as a bulk transition. It also showed a hysteretic behavior, although the coercive force was very small (less than 20 Oe). The saturation value of the magnetization curve at 409 mK was ca. 70% of the corresponding value at 80 mK. This indicates that about 30% of the spins still fluctuate thermally at 409 mK.
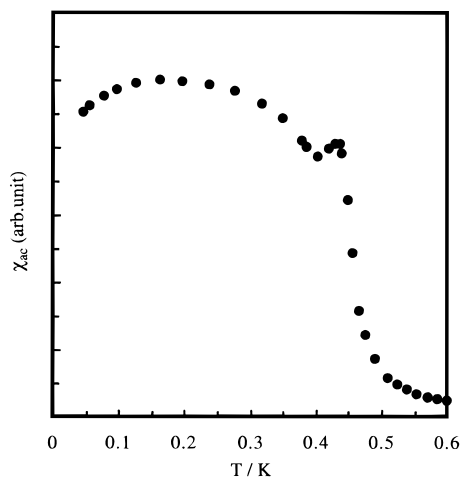
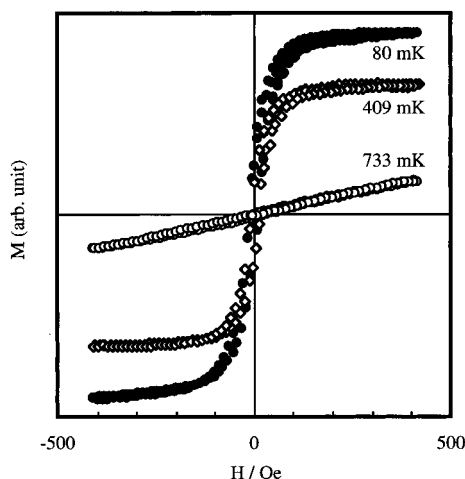**Figure 7.** Ac susceptibility of α-HQNN at lower temperatures.

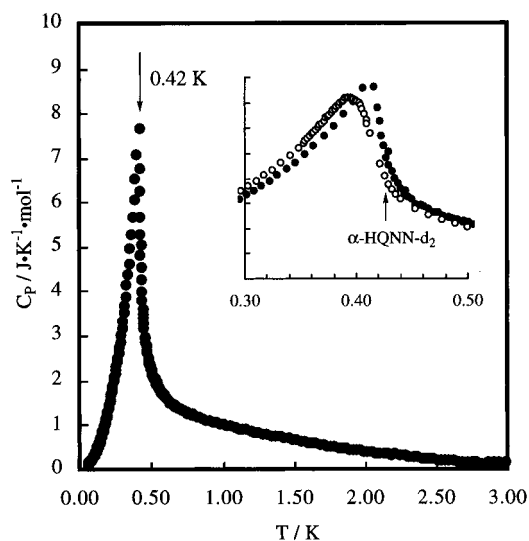**Figure 8.** Magnetization curves of α-HQNN measured at 733, 409, and 80 mK.

Figure 9. Temperature dependence of heat capacity of α-HQNN. Insert shows the change of the heat capacity by deuteration at lower temperatures.

The temperature dependence of the heat capacity, C_p, around the T_C is depicted in Figure 9. The heat capacity exhibited a λ-shaped anomaly with a peak at 0.42 K. The associated entropy change was evaluated to be 5.4 J·K^{-1}·mol^{-1} by integrating the area of the peak in the $C_p/T-T$ plot, and the obtained value was in accord with the theoretical value of R ln
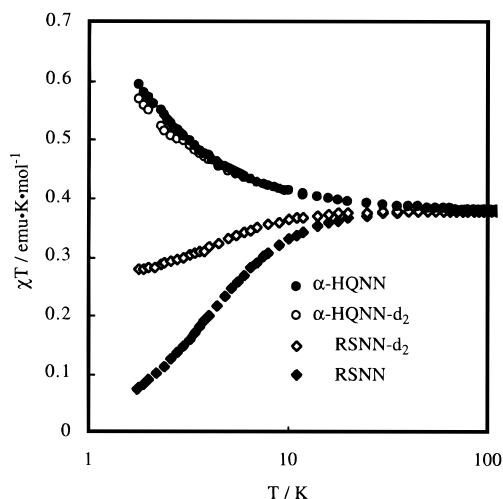

Figure 10. Magnetic susceptibility of the deuterated samples of α-HQNN and RSNN together with the data of non-deuterated samples. The experimental error in the SQUID measurement is in the range of 0.01%.

2 = 5.76 J·K^{-1}·mol^{-1} within experimental error. The result gives independent evidence for the bulk nature of the phase transition.

Magnetic Property of Deuterated α-HQNN, β-HQNN, and RSNN. Deuterated α-HQNN, β-HQNN, and RSNN were prepared by recrystallization from ethanol-d_1. The α- and β-phase crystals of HQNN were obtained by using a small amount of the corresponding seed crystals.

In α-HQNN-d_2, the IR spectrum of the crystal shows peaks at 2434 and 1030 cm^{-1} which are assignable to the O–D stretching and the bending modes, respectively. Furthermore, there is a broad peak at 1800–2100 cm^{-1} assignable to the hydrogen-bonded O–D stretching of the intramolecular hydrogen bond. These results suggest that both hydroxy groups are deuterated. The percentage of deuteration of the sample was estimated to be more than 70% on the basis of the intensities of IR absorption peaks. The ratios of deuteration of β-HQNN and RSNN were also estimated to be more than 80% and 60%, respectively.

The magnetic susceptibility of the deuterated samples was measured at the temperatures ranging between 1.8 and 280 K, using a SQUID magnetometer (main field 5 kOe). The χT values of these samples at an ambient temperature assure the purity of the samples. When the temperature dependence of the magnetic susceptibility of α-HQNN-d_2 was compared with the non-deuterated sample, the χT value at 1.8 K was decreased from 0.600 to 0.570 emu·K·mol^{-1} (Figure 10). The effect of deuteration was more pronounced in the case of RSNN. Upon deuteration, the χT value at 1.8 K increased from 0.078 to 0.280 emu·K·mol^{-1}, indicating the significant decrease in the anti-ferromagnetic interaction. In β-HQNN, the effect of deuteration on the magnetic interaction is found to be negligible.

The temperature dependence of the heat capacity of 70% deuterated α-HQNN-d_2 showed a broad λ-shaped anomaly in the temperature range 0.38–0.40 K (see insert in Figure 9). The peak position was shifted to the lower temperature side compared with the non-deuterated sample.

Discussion

Molecular Design of Free Radicals Having Hydrogen-Bonding Sites. We designed phenyl nitronyl nitroxide derivatives substituted with hydroxy groups (HQNN and RSNN) to form hydrogen-bonded crystals. The spin distribution of phenyl nitronyl nitroxide (PhNN) has been investigated in detail by
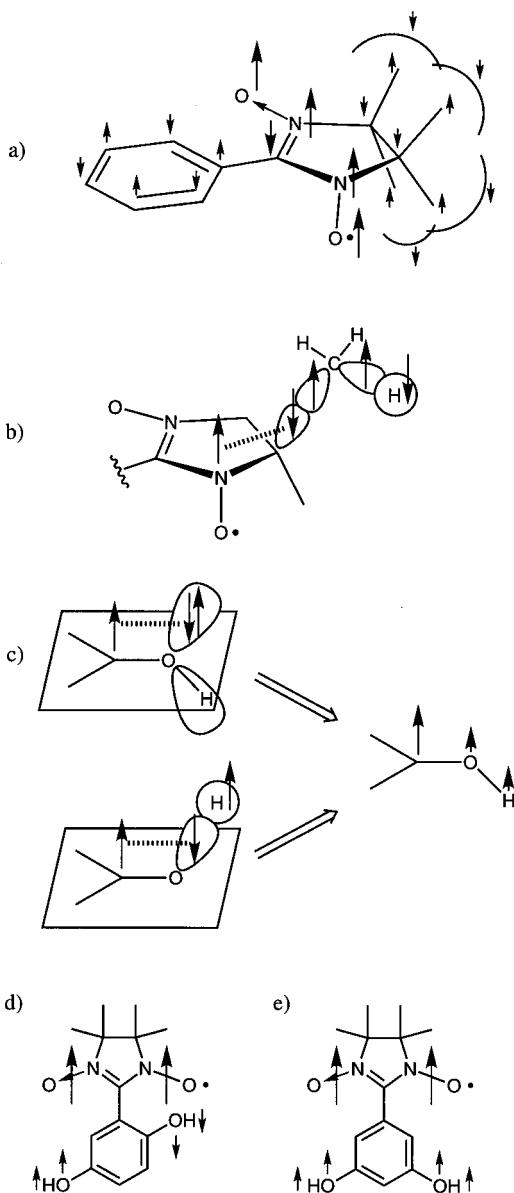
Figure 11. (a) Spin distribution on the phenyl nitronyl nitroxide. (b) Spin polarization at the methyl hydrogen of nitronyl nitroxide derived from a hyperconjugation between the π radical and the C—C bond. (c) Spin-induction mechanism at an oxygen atom and a hydrogen atom of the hydroxy group. (d) Signs of spin densities on the hydroxy groups of HQNN. (e) Signs of spin densities on the hydroxy groups of RSNN.

ESR,[17] NMR,[18] neutron diffraction experiment,[19] and theoretical calculation.[20] The characteristics of the spin distribution are as follows (Figure 11a): First, most of the spin densities are equally shared by two NO groups. Second, a large negative spin density is observed on the C1 atom between the two NO groups. Third, an alternation in the spin densities on the carbon atoms of the phenyl ring is noted. Fourth, the methyl protons of the NN groups have significant negative spin densities, derived from the positively polarized methyl carbons (Figure 11b). Since the g values and the hfs parameters, determined by ESR spectra of HQNN and RSNN in benzene solution, are

(17) Neely, J. W.; Hatch, G. F.; Kreilick, R. W. *J. Am. Chem. Soc.* **1974**, *96*, 652–656.

(18) D'Anna, J. A.; Wharton, J. H. *J. Chem. Phys.* **1970**, *53*, 4047–4052.

(19) Zheludev, A.; Barone, V.; Bonnet, M.; Delley, B.; Grand, A.; Ressouche, E.; Rey, P.; Subra, R.; Schweizer, J.; *J. Am. Chem. Soc.* **1994**, *116*, 2019.

(20) Yamaguchi, K.; Okumura, M.; Nakano, M. *Chem. Phys. Lett.* **1992**, *191*, 237.

practically the same as those of PhNN and other nitronyl nitroxide derivatives, the spin densities of HQNN and RSNN are practically the same as those of PhNN.

In HQNN, two hydroxy groups are introduced at 2′- and 5′-positions carrying negative and positive spin densities, respectively. The signs of spin densities on the oxygen and the hydrogen atoms of the hydroxy group should be same as the *ipso* carbon atom because of the contribution of the hyperconjugation between the π-spin on the *ipso* carbon atom and the lone pairs of electrons of the oxygen atom or the OH bond (Figure 11c).[21] Accordingly, the spin distribution on the hydroxy groups of HQNN should be depicted as shown in Figure 11d.[22] If the intermolecular hydrogen bond is formed between these two sites, the spin polarization may be transmitted along the hydrogen bond, leading to the ferromagnetic intermolecular interaction. On the other hand, the magnetic interaction in RSNN may be opposite to the previous case because the hydroxy groups are introduced at 3′- and 5′-carbons which carry positive spin densities (Figure 11e).

Correlation between the Crystal Structures and the Magnetic Properties of α-HQNN, β-HQNN, and RSNN. In the α-phase crystal, the one-dimensional hydrogen-bonded chains are constructed through the intermolecular hydrogen bond between the phenolic hydroxy groups at C5′ and C2′ carbons belonging to the neighboring molecules, respectively (Figure 3a). Since the signs of spin densities at these sites are opposite, the spin polarization should be transmitted ferromagnetically in accord with the McConnell mechanism (Figure 12a). In fact, the intermolecular ferromagnetic interaction was detected by magnetic measurements in this crystal.

It is to be noted that there is a bifurcated hydrogen-bonded pair connecting the two parallel hydrogen-bonded chains. In this pair, the intermolecular distance between the oxygen atoms of the NN groups O(2(a))−O(2(b)) is as short as 3.16 Å (Figure 3c). Although such a proximity of radicals usually causes the antiferromagnetic interaction, the experimental result suggests the presence of ferromagnetic interaction even at this site. In this respect, the ferromagnetic interaction through the hydrogen bond is considered to predominate over the antiferromagnetic through-space NO···ON interaction (Figure 12b). The presence of the ferromagnetic intermolecular interaction in this contact was reproduced through theoretical calculation by Yamaguchi *et al.*[23] When the *o*-hydroxy groups are removed, the model system exhibits a large antiferromagnetic intermolecular interaction due to the close contact of the NO groups. This result is strong evidence for the transmittance of ferromagnetic coupling through the hydrogen bonds.

Although one may predict the low dimensionality in the magnetic interaction for α-HQNN due to the hydrogen-bonded

(21) The spin density on the hydroxy group in the model spin system, CH$_2$OH radical, was calculated by MNDO-PM3/UHF using MOPAC version 6.0 (QCPE No. 445: Stewart, J. J. *QCPE Bull.* **1990**, *10* (4), 86). When the dihedral angel, $\theta = \angle$HCOH, is 0°, the spin density on the hydrogen atom of the hydroxy group is nearly equal to 0, and increased to 0.08 at 90° following the sin$^2 \theta$ relation. On the contrary, the spin density on the oxygen atom is 0.10 at 0°, and it decreases following the cos$^2 \theta$ relation. It falls to −0.04 at 90° crossing zero at around 60°. According to this result, both the hydrogen and the oxygen atoms of the hydroxy group have the same sign of spin densities as the *ipso* carbon atom in the dihedral angle range of 0°−60°. Such a result does not conflict with the qualitative explanation in the text.

(22) Recently, the spin densities on the hydroxy groups of HQNN were determined by the high-resolution solid state NMR experiment. The result is consistent with result which is described in this paper.: Takeda, S.; Maruda, G.; Oda, A.; Yamaguchi, K.; Matsushita, M. M.; Izuoka, A.; Sugawara, Symposium on Molecular Structure, Fukuoka, Japan, 1996, Abstr. 2P3a57, p 312.

(23) Oda, A.; Kawakami, T.; Takeda, S.; Mori, W.; Matsushita, M. M.; Izuoka, A.; Sugawara, T.; Yamaguchi, K. *Mol. Cryst. Liq. Cryst.*, in press.
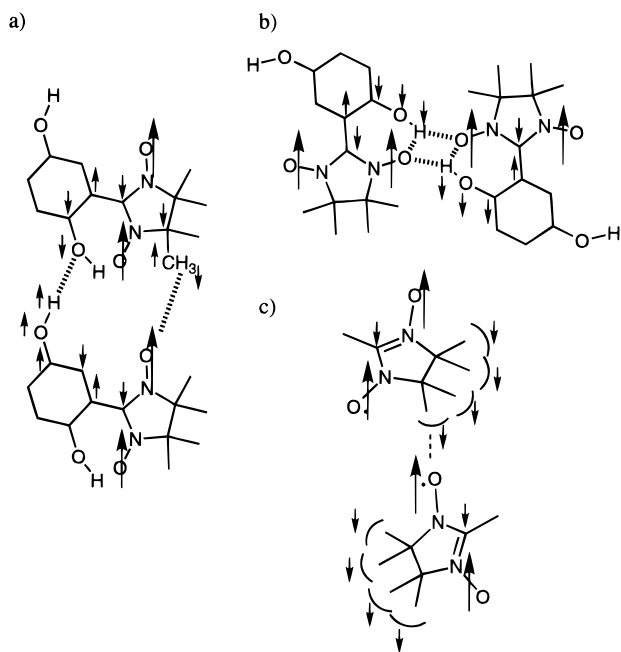
Figure 12. Spin transmission along the hydrogen bond in α-HQNN. (a) Ferromagnetic interaction along the hydrogen-bonded chain. The CH···ON type contact along this direction also contribute to the ferromegnetic interaction. (b) Ferromagnetic interaction between the doubly bifurcated hydrogen-bonded pair. (c) Ferromagnetic interaction through a CH···ON type contact within the *ab*-plane.

Figure 13. Schematic drawing of the spin system of α-HQNN. Ferromagnetically coupled dimeric pair surrounded by six neighboring pairs.

crystal structure, the magnetic interaction in HQNN was interpreted to be of a three-dimensional character, judged from the heat capacity data. The result suggests that the magnetic interaction along the hydrogen-bonded chain is not exceptionally strong, but comparable to other interactions. Therefore one should examine the magnetic interactions other than that through the hydrogen bonds. When the crystal structure of α-HQNN is examined more closely, one may notice that the oxygen atom of the NN group is located close to one of the methyl hydrogen atoms of the NN group of the adjacent molecule. The methyl hydrogen atoms, in fact, are found to be spin-polarized negatively.[17−20] Since the carbon atom of the methyl group, which is parallel to the p orbital of the nitronyl nitroxide moiety, has the positive spin density, presumably through the hyper-conjugative mechanism, the hydrogen atoms of the methyl group are assumed to be spin-polarized negatively (Figure 11b). Thus, the CH···ON interaction should increase the dimensionality of the magnetic interaction in this crystal (Figure 12c). Incidentally, this type of contact is also observed in the hydrogen-bonded chain of α-HQNN (Figure 3b). Such contact should cooperate with the intermolecular hydrogen bond to reinforce the ferromagnetic interaction along this chain (Figure 12a).

This CH···ON interaction has been already pointed out in several cases.[4,13,14,24] Veciana *et al.* discovered that *o*-hydroxyphenyl nitronyl nitroxide (*o*-HPNN) exhibits a ferromagnetic phase transition at 0.4 K.[14a] *o*-HPNN does not form a one-dimensional hydrogen-bonded chain, due to the lack of an additional hydroxy group at 5′-position compared with HQNN. The three-dimensional ferromagnetic interaction observed in this crystal is ascribed to the CH···ON type interaction between methyl group and the nitronyl nitroxide group of the adjacent molecule. Nogami *et al.* also reported that the ferromagnetic interaction in the TMPOs may be caused by the contact between
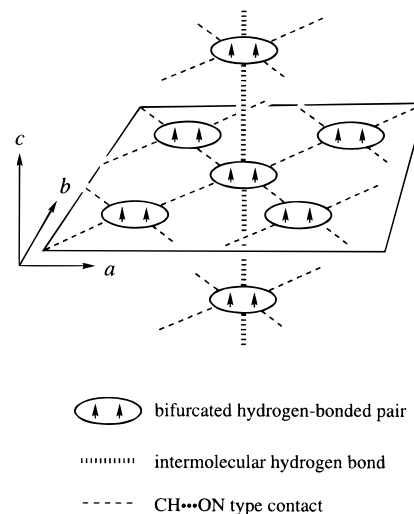
the methyl hydrogen atoms having negative spin densities and the oxygen atoms of the nitroxyls having large positive spin densities.[4]

Since the temperature dependence of α-HQNN was best interpreted by the ST model with the positive Weiss temperature, the magnetic interaction may be best interpreted by the following model. The strong dimeric interaction may be assigned to the pair of HQNN connected by the bifurcated hydrogen bond. The ferromagnetically coupled pair is, then, surrounded by neighboring pairs three-dimensionally as schematically shown in Figure 13. When the crystal structure is examined more closely, it is noted that one pair is surrounded by six neighboring pairs. Two pairs are located along the hydrogen bond. The other four pairs are located in the *ab*-plane through CH···ON interactions. Such a molecular packing is consistent with the experimental data (*vide infra*).

In β-HQNN, the oxygen atom of the NN group is hydrogen-bonded to the phenolic OH group of the adjacent molecule (Figure 4). It is energetically favorable that the spins at the interacting site are aligned in an antiparallel manner. Since the signs of the spin densities at the oxygen atom of the NN moiety and the OH group at C5′ position are the same, the intermolecular interaction between these two sites leads to an antiferromagnetic interaction. In fact, the antiferromagnetic interaction is detected in the low-temperature region ($T < 3$ K). On the other hand, the magnetic interaction at the higher temperature region ($T > 3$ K) is ferromagnetic. This ferromagnetic interaction cannot be interpreted by the coupling through the hydrogen bond but can be rationalized by the through-space π−π type interaction between the oxygen atom and the carbon atom of the NN groups of the molecule below, the distance between O2 and C1 being 3.78 Å (overlap mode of A in Figure 4c). As these two sites have large and opposite signs of spin densities, this contact satisfies the McConnell's situation (Figure 14b). Similar orientation in other ferromagnetic NN crystals has been reported and discussed by Rey *et al.*[25] Ferromagnetic interaction from this interaction in β-HQNN is considered to be dimeric on the basis of the crystal structure. Thus, the structural feature is consistent with the ST model with the positive intradimer interaction, accompanied by the negative Weiss temperature.

Coexistence of ferro- and antiferromagnetic interaction was also recognized in the crystal of RSNN, as in the case of β-HQNN. The origin of these magnetic interactions resembles

---

(24) Computational studies of the intermolecular magnetic interaction in the hydrogen-bridged nitroxides were performed by Yamaguchi *et al.*, see: Kawakami, T; Takeda, S; Mori, W; Yamaguchi, K. *Chem. Phys. Lett.* **1996**, *261*, 129−137 and references therein.
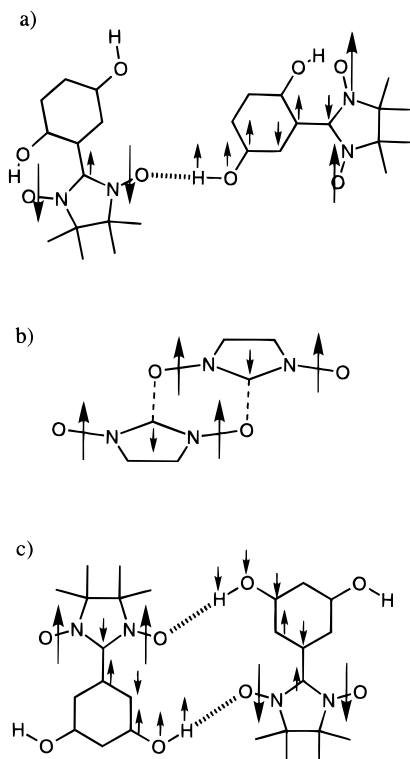
Figure 14. Plausible mechanism of spin transmission of β-HQNN and RSNN: (a) Antiferromagnetic interaction along hydrogen bond in β-HQNN, (b) Spin coupling between two nitronyl nitroxides through the $\pi-\pi$ type interaction, (c) Antiferromagnetic interaction along the doubly hydrogen bonded chain in RSNN.

that of β-HQNN. Namely, the dimeric ferromagnetic interaction of RSNN originates from the through-space π-type interaction within the dimer along the stacking direction (Figure 5c). The close contact is recognized between the oxygen atom of the NN group and the C1 of the NN group of the molecule underneath (mode A overlap). On the other hand, the strong antiferromagnetic interaction is observed in RSNN. This interaction may be resulted from the double intermolecular hydrogen bonds between the hydroxy groups substituted at C(3') or C(5') positions and the oxygen atoms of the NN groups (Figure 5a), because the magnetic interaction through these hydrogen bonds is antiferromagnetic as described in Figure 14c. This antiferromagnetic interaction should be enhanced significantly because of the presence of the double hydrogen bonds. One may notice that the double hydrogen-bonded pattern observed in RSNN resembles that of α-HQNN, although the nature of the intermolecular magnetic interaction is the reverse. The absolute degree of the magnetic interaction of RSNN ($|\theta|$ = 4 K), however, is much stronger than that of α-HQNN ($|J|$ = 0.95 K). The reason may be ascribed to the geometrical difference related to the double hydrogen bonds in these two crystals. In the case of α-HQNN, two NO groups are arranged in proximity by the double bifurcated hydrogen bonds. The close contact of the NO groups in α-HQNN is considered to cancel the ferromagnetic intermolecular interaction through the hydrogen bonds. On the other hand, two NO groups in RSNN are located far apart in the double hydrogen bonds. Thus, these experimental results may be considered as evidence for the transmission of the spin polarization through the hydrogen bonds.

Dimensionality of Magnetic Interaction of α-HQNN. Dimensionality of the magnetic interaction is closely related to the mechanism of the spin ordering. In α-HQNN, the anomaly in the heat capacity is observed at 0.42 K (Figure 9). The ratio

Table 8. Ratio of T_C/θ and the Entropy of the Spin System (S_C) in the Lower Temperature Region than T_C and that ($S_\infty - S_C$) in the Higher Temperature Region than T_C[a]

model or crystal	T_C/θ	S_C, %	$S_\infty - S_C$, %
mean field	1	100	0
Ising s.c. ($Z = 6$)	0.75	81	19
Ising diamond ($Z = 4$)	0.67	74	26
Heisenberg f.c.c	0.67	67	33
Heisenberg b.c.c	0.63	65	35
Heisenberg s.c.	0.56	62	38
α-HQNN	0.56	60	40

[a] S_C: entropy change between 0 K and T_C. S_∞: entropy change of phase transition.

of T_C and θ is known to reflect the dimensionality of the spin interaction.[26] While the ratio (T_C/θ) is equal to 1 in the molecular field approximation, it decreases together with a decrease in dimensionality of the spin–spin interaction. The ratio for α-HQNN is estimated to be 0.51 (T_C = 0.42 K, θ = 0.82 K), and the value is close to that of the three-dimensional Heisenberg model (T_C/θ = 0.56 for a simple cubic lattice).

The relative ratio of the entropy in the temperature region lower than T_C (S_C) and that in the higher region ($S_\infty - S_C$) is evaluated to be 0.60–0.40. Since the ratio should increase accompanied by the decrease in the dimensionality of the spin–spin interaction, it also serves as a scale to estimate the dimensionality of the spin system.[26] The obtained value suggest that the dimensionality of α-HQNN is close to the three-dimensional Heisenberg model ($z = 6$) as shown in Table 8. These results also substantiate the picture of the spin system discussed previously.

Effect of Deuteration on the Magnetic Property of α-HQNN, β-HQNN, and RSNN. Generally, the H–X bond distance is shortened by substituting hydrogen with deuterium. In the case of a hydrogen bond, the shortening of the O–D bond causes an elongation of the hydrogen bond distances.[27] If the hydrogen bond contributes to the transmission of the spin polarization, the deuteration should affect the degree of the intermolecular magnetic interaction. In fact, the apparent ferromagnetic interaction of α-HQNN decreased upon deuteration of the hydroxy groups. Namely, the χT value at 1.8 K decreases by 5% (from 0.60 to 0.57 emu·K·mol^{-1}) for the 70% deuterated sample.

In β-HQNN, the effect of deuteration on the magnetic interaction is found to be negligible. Since the through-space interaction predominates over the interdimer interaction through the hydrogen bond, the result is not an unexpected one.

The effect of deuteration on RSNN is much more pronounced than that on β-HQNN. The magnetic susceptibility increases by 350% (from 0.08 to 0.28 emu·K·mol^{-1}) at 1.8 K for the 60% deuterated sample. This is reasonable because the hydrogen bonds in RSNN are stronger and doubly-formed.

Although the detailed discussion on the structural change in the deuterated sample should await determination of the crystal structure, the change in the magnetic interactions in these crystals (α-HQNN, β-HQNN, and RSNN) is consistent with the interpretation that the magnetic interaction is transmitted through the hydrogen bond.

The maximum of the heat capacity was shifted to the lower temperature side, and the peak was broadened compared with that of the hydrogen counterpart. The shift to the lower temperature indicates the decrease in the magnetic interaction

(25) Panthou, F. L.; Luneau, D.; Laugier, J.; Rey, P. *J. Am. Chem. Soc.* **1993**, *115*, 9095.
(26) Jongh, L. J.; Miedema, A. R. *Adv. Phys.* **1974**, *23*, 1.
(27) Ichikawa, M. *Acta Crystallogr.* **1978**, *B34*, 2074–2080.

Scheme 1

2(a 2,5 b 3,5)   3(a 2,5 b 3,5)   1(a 2,5 = HQNN
                                                                   b 3,5 = RSNN)
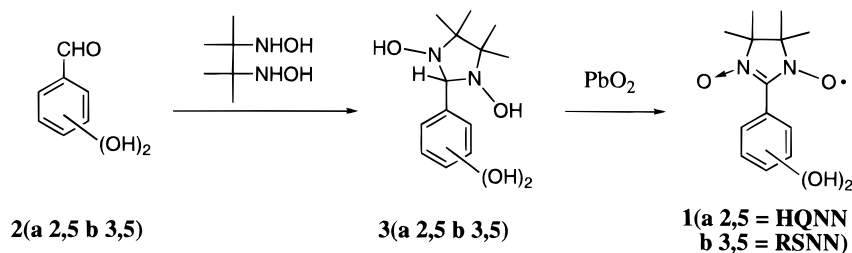
of the deuterated sample. The broadening of the peak may arise from the inhomogeneous distribution of the deuterated hydroxy groups due to the incomplete deuteration.

Effect of Introduction of Hydrogen Bonds on the Magnetic Property of Phenyl Nitronyl Nitroxides. The intermolecular ferromagnetic interaction was detected in the crystals of both α-HQNN and β-HQNN in terms of the temperature dependence of the magnetic susceptibility. When the other phenyl nitronyl nitroxides with hydroxy group(s) are taken into account, the ferromagnetic interaction is detected in six cases.[13,14] Judging from these results, introduction of hydroxy groups to phenyl nitronyl nitroxides may contribute not only to constitute appropriate hydrogen-bonded crystal structures but also to transmit the spin polarization intermolecularly. The correlation between the magnetic property and the hydrogen bond pattern of α-HQNN, β-HQNN, and RSNN turned out to be rationalized by McConnell's mechanism. In the bifurcated hydrogen bond of α-HQNN, the intermolecular magnetic interaction might have become antiferromagnetic, unless the ferromagnetic interaction through hydrogen bonds predominates over the antiferromagnetic interaction caused by the close contact of the NO groups. Thus, the presence of the ferromagnetic route through the hydrogen bond was proved experimentally. On the other hand, the CH···ON interaction and the $\pi-\pi$ interaction cannot be ignored. Utilization of the latter interactions, however, is difficult in the crystal engineering. On the contrary, the hydrogen bond is powerful and predictable for constructing crystal structures and also effective in aligning electron spins intermolecularly based on the McConnell mechanism. Furthermore, hydrogen bonds can be formed between such various functional groups as hydroxyenones, carboxy, amido, etc. Thus the hydrogen bond may be applicable widely to control the molecular arrangement of organic radicals. Although the crystal design for organic ferromagnets is extremely difficult at the present stage, the hydrogen bond methodology seems to be promising in this respect.

Conclusion

We designed and prepared nitronyl nitroxide derivatives carrying a hydroquinone or a resorcinol moiety (HQNN and RSNN) to form hydrogen-bonded crystals. In all cases, the magnetic behaviors are consistent with McConnell's theory, when the spin densities at the interacting sites through hydrogen bonds are taken into account. Among them, α-HQNN turned out to exhibit a ferromagnetic phase transition at 0.5 K and it is a first organic ferromagnet which is constructed by hydrogen bonds.[12] To connect the spin polarized sites more decisively in an appropriate mode, it may be effective to utilize hydrogen bonds at multisites. The utilization of hydrogen bonds may also be effective in controlling the magnetic property through the switching of hydrogen bonds.[28] Although it is crucial to induce significant spin densities on the hydrogen-bonding sites, the

hydrogen bond may be utilized as the "spin coupler". Thus it may play an important role in designing various artificial spin systems.[1]

Experimental Section

Preparation. Two new nitronyl nitroxide derivatives were synthesized from corresponding formyl compounds as shown in Scheme 1 according to the ordinary method.[29]

HQNN (2-(2′,5′-Dihydroxyphenyl)-4,4,5,5-tetramethyl-4,5-dihydro-1H-imidazolyl-1-oxyl 3-Oxide) (1a). In a 100 mL round-bottom flask were placed 1.94 g of 2,5-dihydroxybenzaldehyde (**2a**) (14 mmol), 1.80 g of 2,3-dimethyl-2,3-dihydroxylaminobutane[30] (12 mmol), 0.07 g of 2,3-dimethyl-2,3-(dihydroxylaminium)butane sulfonate (catalyst), and 4 g of crushed 3Å molecular sieves under a nitrogen atmosphere. To this mixture was added 50 mL of benzene containing 5% of methanol. After stirring for 4 days, the solvent was removed by evaporation, 50 mL of CHCl₃ was added, and the mixture was filtered. The residue was washed with CHCl₃ twice over a filter, and the condensation product was extracted with THF. After evaporation, the cyclic bis(hydroxylamine) (**3a**) was obtained as white powder: 2.86 g (88%). NMR (270 MHz, acetone-d_6): δ = 7.42 (1H, br.s, −OH), 6.71 (1H, d, J = 2.93 Hz, Ar-H), 6.61 (1H, dd, J = 2.93, 8.79 Hz, Ar-H), 6.50 (1H, d, J = 8.42 Hz, Ar-H), 4.68 (1H, s, methine-H), 1.20 (6H, s, methyl-H), 1.14 ppm (6H, s, methyl-H). Under a nitrogen atmosphere, 208 mg of **3a** (cyclic bis(hydroxylamine)) (7.8 mmol) was placed in a 50 mL round-bottomed flask. Dried THF of 10 mL was added, and the mixture was stirred at room temperature. A mixture of 1.0 g of PbO₂ and 200 mg of crushed molecular sieves (3A) was added into the solution and stirred for 10 min. The solution was filtered off through a Celite pad to yield a dark blue solution. After condensation, the oxidized product was purified by silica-gel column chromatography with diethyl ether as an eluant. Fractions colored blue were collected and dried over sodium sulfate and filtered off. A purple oil (HQNN, **1a**) of 170 mg was obtained by removing the solvent; 88% yield. ESR (benzene): g = 2.0061, a_N = 0.756 mT (2N). Mass (FAB): Obsd (M + 1)⁺ = 266 (calcd C₁₃H₁₇N₂O₄ = 265). UV (THF): λ_{max} = 347 (ϵ > 7000), 580 (ϵ = 410), 630 nm (ϵ = 270). **Crystallization of HQNN.** A purple oil of HQNN was mixed with 30 mL of diethyl ether. Then the dark blue solution was stored in a refrigerator (≈4 °C) under a nitrogen atmosphere. After 4 h, block-shaped blue-purple crystals (α-phase), ca. 0.2 × 0.4 × 0.2 mm in size, were obtained. When the solution was stored in a freezer (≈−10 °C), needle-shaped crystals (β-phase) were obtained. Both phases can be obtained selectively by using a seed crystal at room temperature. **α-phase crystal.** IR (KBr): 3270 (OH), 1480, 1332 cm⁻¹ (nitronyl nitroxide). E.A. calcd. for C₁₃H₁₇N₂O₄: C, 58.85; H, 6.46; N, 10.56. Found: C, 58.89; H, 6.47; N, 10.54. Mp: 109 °C (dec). **β-phase crystal.** IR (KBr): 3320 (OH), 1489, 1456, 1426, 1326 cm⁻¹ (nitronyl nitroxide). E.A. calcd for C₁₃H₁₇N₂O₄: C, 58.85; H, 6.46; N, 10.56. Found: C, 58.78; H, 6.46; N, 10.53. Mp: 108 °C (dec).

RSNN (2-(3′,5′-Dihydroxyphenyl)-4,4,5,5-tetramethyl-4,5-dihydro-1H-imidazolyl-1-oxyl 3-Oxide) (1b). In a 30 mL round-bottom flask were placed 0.244 g of 3,5-dihydroxybenzaldehyde (**2b**) (1.8 mmol), 0.243 g of 2,3-dimethyl-(2,3-dihydroxylamino)butane (1.7 mmol), 66 mg of 2,3-dimethyl-2,3-(dihydroxylaminium)butane sul-

(28) Byrn, S. R.; Curtin, D. Y.; Paul, I. C. *J. Am. Chem. Soc.* **1972**, *94*, 890−898.

(29) (a) Osiecki, J. H.; Ullman, E. F. *J. Am. Chem. Soc.* **1968**, *90*, 1078. (b) Ullman, E. F.; Osiecki, J. H.; Boocock, D. G. B.; Darcy, R. *J. Am. Chem. Soc.* **1972**, *94*, 7049.

(30) Lamchen, M.; Mittag, T. W. *J. Chem. Soc. C* **1966**, 2300.

fonate, and 1 g of crushed molecular sieves (3A), under a nitrogen atmosphere. To this mixture was added 20 mL of benzene containing 5% of methanol. After stirring 3 days, the solvent was removed by evaporation. The residue was washed with $CHCl_3$ twice over a filter, and the crude condensation product was extracted with THF. After evaporation, the cyclic bis(hydroxylamine) (**3b**) was obtained as white powder: 0.371 g (83%). NMR (270 MHz, DMSO-d_6): δ = 8.96 (2H, d, J = 3.3 Hz, −OH), 7.66 (2H, d, J = 3.48 Hz, N-OH), 6.37 (2H, d, J = 2.38 Hz, Ar-H), 6.07 (1H, s, Ar-H), 4.27 (1H, d, methine-H), 1.02 (12H, t, methyl-H). Under a nitrogen atmosphere, 0.371 g of the cyclic bis(hydroxylamine) (1.38 mmol) was placed in a 100 mL round-bottomed flask. Dried THF of 60 mL was added into the flask, and the mixture was stirred. A mixture of 2.5 g of PbO_2 and 1 g of crushed molecular sieves (3A) was added into the solution, and the mixture was stirred for 4 h. The solution was filtered off through a Celite pad to yield a dark blue solution. After condensation, the oxidized product was purified by silica-gel column chromatography with ethyl acetate as an eluant. A blue fraction was collected and dried over sodium sulfate and filtered off. The obtained crude crystals were dissolved in ethyl acetate and stored in refrigerator ($\approx$4 °C) under a nitrogen atmosphere. Blue plates were obtained: 170 mg (46%). IR (KBr): 3311, 3207(OH), 1372, 1343 cm^{-1}(nitronyl nitroxide). E.A. calcd for $C_{13}H_{17}N_2O_4$: C, 58.85; H, 6.46; N, 10.56. Found: C, 58.63; H, 6.42; N, 10.30. Mp: 75 °C. ESR (benzene): g = 2.0063, a_N = 0.748 mT (2N).

X-ray Data Collection and Structure Determination. The crystal structures of both phases of HQNN and RSNN were revealed by X-ray crystallography. Crystals were mounted on a Rigaku AFC-5 four-circle diffractometer equipped with graphite-monochromatized Mo Kα radiation. The unit cell parameters were obtained by a least-square fit of the automatically centered setting from 25 reflections. In all cases, the positions of non-hydrogen atoms were obtained by direct methods using SAPI-85[31] or SHELXS-86[32] packages. The positions of hydrogen atoms were introduced by difference Fourier maps. Anisotropic thermal factors for all non-hydrogen atoms and isotropic thermal factors for all hydrogen atoms were applied for refinement by using UNICS-III system.[33] The crystallographic parameters are listed in Table 2. Atomic coordinates, bond lengths and angles, and thermal parameters were deposited at the Cambridge Crystallographic Data Center. α-HQNN. A bluish purple block crystal of the α-phase HQNN with dimensions of 0.32 × 0.32 × 0.28 mm was used for data collection. The intensity data were measured at ambient temperature; ω scan (4° < 2θ < 55°), scan speed 4 deg·min^{-1}, −19 < h < 19, 0 < k < 16, 0 < l < 9. Three standard reflections (3 0 3, 6 4 0, and 4 5 0) were measured every 200 reflections and showed no significant variations throughout the data collection; of 3452 reflections (4° < 2θ < 55°) measured, 2204 independent reflections (F_o > 3σ(F_o)) were used for analysis (R_{int} = 0.017). Absorption correction was not applied. Anisotropic thermal factors for all non-hydrogen atoms and isotropic thermal factors for hydrogen atoms were used for final refinement; 240 parameters, R = 0.051 and wR = 0.047; w = 1.0 ($|F_o|$ < 20), 0.7 (20 ≤ $|F_o|$ < 60), 200/$|F_o|^2$ (60 ≤ $|F_o|$); S = 0.56; maximum and minimum heights in final difference Fourier syntheses were 0.632 and −0.309 e $Å^{-3}$; max (shift/esd) = 0.161(y of H[O(2')]). β-HQNN. A blue needle of the β-phase HQNN with dimensions of 0.32 × 0.16 × 0.16 mm was used for analysis. The intensity data were measured at ambient temperature; ω scan (4° < 2θ < 55°), scan speed 4 deg·min^{-1}, −9 < h < 12, 0 < k < 18, 0 < l < 12. Three standard reflections (1 4 1, 0 0 2, and 4 0 1) were measured every 200 reflections and showed no significant variations throughout the data collection; 3330 reflections (4° < 2θ < 55°) measured, 1596 independent reflections (F_o > 3σ(F_o)) were used for analysis (R_{int} = 0.022). Absorption correction was not applied. Anisotropic thermal factors for all non-hydrogen atoms and isotropic thermal factors for hydrogen atoms were used for final refinement; 240 parameters, R = 0.049 and wR = 0.048; w = 1.0 ($|F_o|$ < 50), 200/

$|F_o|^2$ (50 ≤ $|F_o|$); S = 0.73; maximum and minimum heights in final difference Fourier syntheses were 0.350 and −0.272 e $Å^{-3}$; max (shift/esd) = 0.223 (B of H[C(4)]1). RSNN. A blue plate crystal of RSNN with dimensions of 0.40 × 0.36 × 0.16 mm was used for analysis. The intensity data were measured at ambient temperature; ω scan (4° < 2θ < 55°), scan speed 4 deg·min^{-1}, −10 < h < 12, 0 < k < 25, 0 < l < 9. Three standard reflections (5 3 2, 2 10 0, and 4 4 3) were measured every 200 reflections and showed no significant variations throughout the data collection; of 3316 reflections (4° < 2θ < 55°) measured, 2220 independent reflections (F_o > 3σ(F_o)) were used for analysis (R_{int} = 0.025). Absorption correction was not applied. Anisotropic thermal factors for all non-hydrogen atoms and isotropic thermal factors for hydrogen atoms were used for final refinement; 240 parameters, R = 0.047 and S = 0.58; maxium and minimum heights in final difference Fourier syntheses were 0.474 and −0.190 e $Å^{-3}$; max (shift/esd) = 0.044 (x of H[O(4)]).

Magnetic Measurements. ESR spectra were recorded by using a JEOL JES-RE2X X-band (9.4 GHz) spectrometer equipped with a Advantest TR-5212 frequency counter. The magnetic susceptibility of the polycrystalline samples were measured on a Quantum Design MPMS-5S SQUID susceptometer working at the field strength of 0.5 T in the temperature range 1.8−280 K. The contribution of the sample holder and the diamagnetism of the sample were estimated from high-temperature extrapolation and then substructed to yield a paramagnetic component.

AC Susceptibility and Low-Temperature Magnetization of α-HQNN. The ac susceptibility (χ_{ac}) of α-HQNN was measured down to 40 mK in a ^3He−^4He dilution refrigerator[34] at the ac magnetic field of about 10 mT (127 Hz).[35] The magnetizations at 80, 409, and 733 mK were measured with a standard integration method similar to that described previously.[36]

Heat Capacity of α-HQNN. The heat capacity of α-HQNN was measured in the temperature range 0.057−3.28 K in a ^3He−^4He dilution refrigerator with a usual adiabatic heat pulse method. To obtain information on the spin ordering from the heat capacity data, it is necessary to exclude the phonon contribution from the measured heat capacity data. Since the heat capacity derived from phonon at cryogenic temperatures is proportioned to T^3 according to Debye's approximation, the lattice heat capacity is estimated from the slope of the C_p−T^3 plot. The pure contribution of the spin system was obtained, after substracting the phonon contribution from the overall heat capacity.

Other Instrumentation. An ^1H (270 MHz) NMR spectrum was obtained on a JEOL GSH-270 spectrometer. Infrared spectra and UV−vis absorption spectra were obtained on a Perkin-Elmer 1640 FTIR and Shimazu UV-3100PC, respectively.

Supporting Information Available: Crystallographic details for α-HQNN, β-HQNN, and RSNN, including tables of atomic coordinates and isotropic thermal parameters, bond lengths and angles, and anisotropic thermal parameters (15 pages). See any current masthead page for ordering and Internet access instructions.

JA964083O

(31) Fan, H.; Qian, J.; Yao, J.; Zheng, C.; Hao, Q. *Acta Crystallogr., Sect.* A **1988**, *44*, 691.

(32) Sheldrick, G. M. *Crystallographic Computing 3*; Sheldrick, G. M.; Kruger, C., Goddard, R., Eds. Oxford University Press: Oxford, U.K., 1985; p 175.

(33) Sakurai, T.; Kobayashi, K. *Rep. Inst. Phys. Chem. Res. (Tokyo)* **1979**, *55*, 69.

(34) Ishikawa, M.; Nakazawa, Y.; Takabatake, T.; Kishi, A.; Kato, R.; Maesono, A. *Solid State Commun.* **1988**, *66*, 201.

(35) The ac magnetic field in the χ_{ac} measurement in ref 12 must be corrected to 10 mT.

(36) Ishikawa, M.; Muller, J. *Solid State Commun.* **1978**, *27*, 761.

(37) The crystal structures in this paper are drawn by Moldraw: Molecular graphics for Machintosh: Cense, J.-M. *Tetrahedron Comput. Methodol.* **1989**, *2*, 65−71.